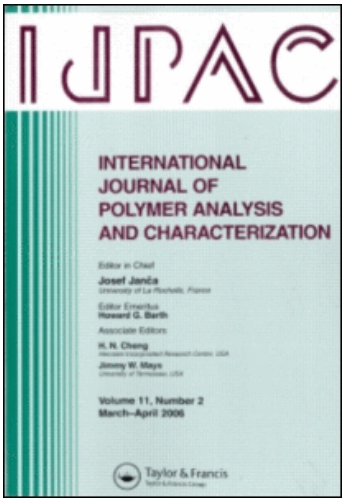

International Journal of Polymer Analysis and Characterization
Publication details, including instructions for authors and subscription information:
http://www.informaworld.com/smpp/title~content=t713646643

Synthesis and Structural Characterization of Polyaniline/Mesoporous Carbon Nanocomposite

Ying He[ab]; Qilin Cheng[a]; Vladimir Pavlinek[a]; Chunzhong Li[b]; Petr Saha[a]
[a] Polymer Centre, Faculty of Technology, Tomas Bata University in Zlin, Zlin, Czech Republic [b] Key Laboratory for Ultrafine Materials of Ministry of Education, School of Materials Science and Engineering, East China University of Science and Technology, Shanghai, China

To cite this Article He, Ying , Cheng, Qilin , Pavlinek, Vladimir , Li, Chunzhong and Saha, Petr(2008) 'Synthesis and Structural Characterization of Polyaniline/Mesoporous Carbon Nanocomposite', International Journal of Polymer Analysis and Characterization, 13: 1, 25 — 36
To link to this Article: DOI: 10.1080/10236660701799419
URL: http://dx.doi.org/10.1080/10236660701799419

International Journal of Polymer Anal. Charact., 13: 25–36, 2008

ISSN: 1023-666X print
DOI: 10.1080/10236660701799419

Taylor & Francis
Taylor & Francis Group

Synthesis and Structural Characterization of Polyaniline/Mesoporous Carbon Nanocomposite

Ying He,[1,2] Qilin Cheng,[1] Vladimir Pavlinek,[1] Chunzhong Li,[2] and Petr Saha[1]

[1]Polymer Centre, Faculty of Technology, Tomas Bata University in Zlin, Zlin, Czech Republic

[2]Key Laboratory for Ultrafine Materials of Ministry of Education, School of Materials Science and Engineering, East China University of Science and Technology, Shanghai, China

Abstract: In this work, a new nanocomposite in which polyaniline (PANI) is encapsulated in ordered mesoporous carbon (CMK-3 type) has been synthesized. The aniline monomer was introduced into hosts from the vapor phase to avoid the formation of PANI layers on the outer surface. The structure and morphology of the nanocomposite were characterized by X-ray diffraction (XRD), N_2 adsorption/desorption, FT-IR and Raman spectra, high-resolution transmission electron microscopy (HRTEM), and thermogravimetric analysis (TGA). The results show that PANI is almost formed in the channels of CMK-3 and the nanocomposite retains the ordered mesostructure. Encapsulated PANI exhibits better thermal stability than pure PANI because of confinement effect in the channel

Received 10 September 2007; accepted 11 November 2007.

This work was supported by the Ministry of Education, Youth and Sports of the Czech Republic (MSM 7088352101) and Grant Agency of the Czech Republic (202/06/0419). The authors also wish to thank to the Special Projects for key laboratories in Shanghai (05DZ22302, 06DZ22008) and the Special Projects for Nanotechnology of Shanghai (0552nm001, 0652nm034) and 973 program (2004CB719500).

Address correspondence to Ying He or Chunzhong Li, Key Laboratory for Ultrafine Materials of Ministry of Education, School of Materials Science and Engineering, East China University of Science and Technology, 200237, Shanghai, China. E-mail: rehey@ecust.edu.cn and czli@ecust.edu.cn

system. The conductivity of PANI/CMK-3 nanocomposite containing 8.4 wt% PANI is 0.78 S/cm at room temperature.

Keywords: CMK-3; Mesoporous carbon; Nanocomposite; Conductivity; Polyaniline

INTRODUCTION

Over the past decade, design and fabrication of novel nanostructured materials based on mesoporous silica have attracted wide attention due to the materials' potential applications in separation, catalysis, and photoelectric nanodevices.[1–3] Ordered mesoporous silica materials with large surface area and uniform pore structure make them an ideal host for the synthesis of new nanocomposites. To date, various guest materials including metals, oxides, and polymers have been incorporated into the channels of mesoporous silica.[4–6] More recently, particular attention has been paid to the investigation of ordered mesoporous carbon-supported materials. Ordered mesoporous carbon materials (OMCs), such as CMK-3, exhibit higher surface area, larger pore volume, and higher mechanical stability and electric conductivity than pure mesoporous silica. Therefore, OMCs can also be used as attractive hosts to generate novel composite systems with special properties. In this respect, Zhu and coworkers reported the synthesis of MnO_2 nanoparticles confined in OMCs with highly improved discharge performance.[7] Wikander et al. synthesized a platinum nanoparticle/carbon composite by impregnation using OMCs as the host.[8] Transition metals and metal oxides inside OMCs were successfully prepared by Huwe and Froba[9] In addition, adsorption of organic materials over OMCs and their potential applications were also reported.[10, 11] The above-mentioned work clearly reveals that the properties of OMCs can be influenced by introduction of guest materials. However, one kind of attractive guest material, conducting polymers, has received little attention, with very few reports on the incorporation of conducting polymers into OMCs so far.[12,13] Conducting polymers intercalated into mesoporous silica[14–20] and other hosts[21, 22] with the purpose of improving electrorheological effect and interaction of the π-conjugated networks have been reported. On the other hand, among the conducting polymers, PANI has attracted a great deal of interest in recent years due to its low cost, ease of preparation, excellent environmental stability, and high electrical conductivity. Therefore, encapsulation of PANI into OMCs may give a rise to unique properties of the final composite system.

In this article, a new nanocomposite with semiconducting PANI inside the channels of CMK-3 has been synthesized by adsorption of aniline vapor into the channels and subsequent oxidative polymerization

with $(NH_4)_2S_2O_8$. The structure and morphology of the nanocomposite were characterized by various techniques.

EXPERIMENTAL SECTION

Materials

Aniline (99%, Aldrich, USA) was distilled under reduced pressure. Ammonium persulfate (APS, $(NH_4)_2S_2O_8$, 98%), tetraethyl orthosilicate (TEOS, 98%), Pluronic 123 (P123, $EO_{20}PO_{70}EO_{20}$, $M_w = 5800$), and hydrofluoric acid (HF, 48%) were purchased from Aldrich Chemicals Co. and used as received without further treatment.

Synthesis of PANI/CMK-3 Nanocomposite

The host structure CMK-3 was synthesized using SBA-15 mesoporous silica as the hard template and sucrose as the carbon source, following the procedure reported by Jun et al.[23]; SBA-15 was obtained by the method described by Zhao et al.[24] The process can be described as follows: SBA-15 (1.0 g) was added to a solution of sucrose (1.25 g) and H_2SO_4 (0.14 g) in H_2O (5 g). The mixture was placed in an oven for 6 h at 100°C and another 6 h at 160°C. In order to obtain fully polymerized and carbonized sucrose inside the pores of the silica template, sucrose (0.8 g), H_2SO_4 (0.09 g), and H_2O (5 g) were again added to the above mixture and then dried at 100°C and 160°C. The carbonization was completed by pyrolysis at 900°C under N_2 flow. Finally, the CMK-3 powder was recovered after dissolution of the silica framework in 5% HF solution, followed by filtration, washing with ethanol, and drying at 120°C.

To obtain the PANI/CMK-3 nanocomposites (Figure 1), the CMK-3 sample was suspended above the aniline monomer in a flask under vacuum ($\sim$0.1 Torr) at 30°C for 24 h. The CMK-3-containing aniline was immersed in a solution of APS (2.85 g) in 50 mL of 0.1 M HCl with stirring at 0–5°C for 12 h. The black product was washed several times with deionized water and ethanol and dried in a vacuum oven at 60°C for 24 h. The 8.4 wt% of mass load of PANI in the composite was evaluated by calculating the weight difference of CMK-3. In addition, pure PANI was also prepared following a procedure similar to that described above, i.e., 0.58 mL aniline was dispersed in a solution of APS (2.85 g) in 50 mL of 0.1 M HCl with stirring at 0–5°C for 12 h. The final powder was also washed several times with deionized water and ethanol and dried in a vacuum oven at 60°C for 24 h.

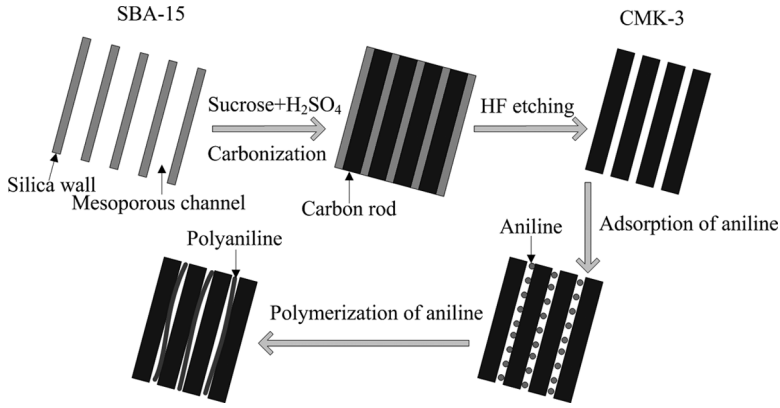

Figure 1. Schematic representation for the synthesis of PANI/CMK-3.

Characterization of Nanocomposite

Small-angle and wide-angle X-ray diffraction (SXRD, WXRD) patterns were determined with a Rigaku D/MAX 2550 V diffractometer using Cu Kα radiation ($\lambda = 1.5406$ Å). N_2 adsorption/desorption isotherms at about -195.6°C were measured using a Micromeritics ASAP 2010 system. The specific surface area and the pore size distribution were calculated by the Barrett-Emmett-Teller (BET) and Barrett-Joyner-Halanda (BJH) methods using the branch of the isotherms. Fourier transform-infrared (FT-IR) spectra were obtained on Nicolet Magna-550 spectrometer. Raman spectra were recorded using a Raman microscope system, the argon-ion laser operated at 514 nm. Thermogravimetric analysis was carried out with a Mettler Toledo TGA/SDTA 851^e at a heating rate of 10°C/min under a purging atmosphere of N_2. The morphology of the nanocomposite was studied using a JEOL JSM-6360LV scanning electron microscope (SEM). High resolution transmission electron micrographs (HRTEM) were taken on a JEM 2100 F electron microscope operating at 200 kV. The DC electrical conductivity of compressed pellets was determined with a Keithley 6517 A electrometer/high resistance meter using the standard four-probe method.

RESULTS AND DISCUSSION

Figure 2 shows the SXRD patterns of SBA-15, CMK-3, and PANI/CMK-3 materials. The SXRD pattern for the as-synthesized sample of SBA-15 exhibits three well-resolved reflections indexed to (100), (110), and (200) planes of the two-dimensional hexagonal space group

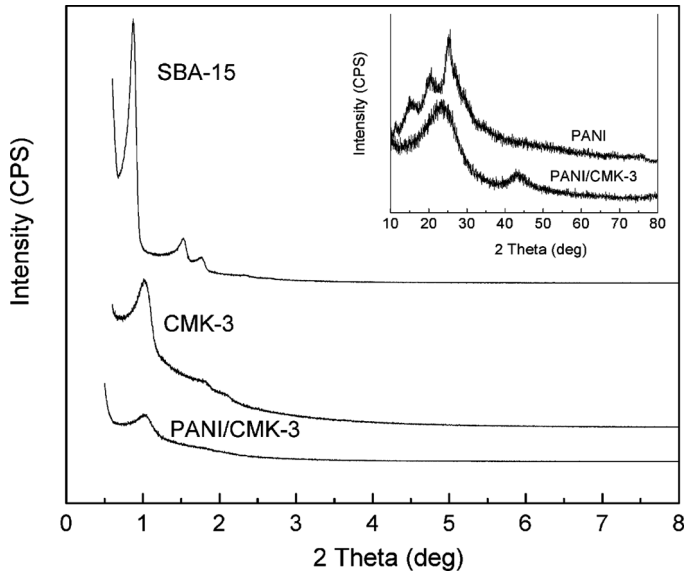

Figure 2. SXRD patterns of SBA-15, CMK-3, and PANI/CMK-3; inset: WXRD patterns of PANI and PANI/CMK-3.

p6mm, which are characteristic of the hexagonal structure of SBA-15 material.[24] Its d (100) value is about 9.3 nm, resulting in a unit cell parameter of $a_0 = 10.7$ nm ($a_0 = 2d_{100}/\sqrt{3}$). The XRD pattern of CMK-3 also displays a strong peak (100) along with weak (110) and (200) peaks similar to the hexagonal structure of the SBA-15 template, suggesting that CMK-3 is a true replica of SBA-15.[23] The cell parameter of CMK-3 ($a_0 = 10.0$ nm) decreases compared to that of SBA-15 due to shrinkage of the carbon framework during carbonization and removal of the silica template.[25] After inclusion of PANI into the pore of the mesoporous carbon, the reflection peak (100) is still clearly shown, thus the PANI/CMK-3 nanocomposite also retains ordered hexagonal mesostructure, which is directly shown in Figure 4(b). Note that a remarkable reduction in the peak intensities is observed with the occupation of pores with PANI in contrast to the pure CMK-3. This is probably caused by the fact that pore filling reduces the scattering contrast between the pores and the walls of the mesoporous material.[26] Moreover, the unit cell constant ($a_0 = 9.8$ nm) of PANI/CMK-3 is lower than that of CMK-3. This can be ascribed to the strong interactions between the PANI chains and the framework walls resulting in contraction of the host lattice upon incorporation of PANI into the pores.

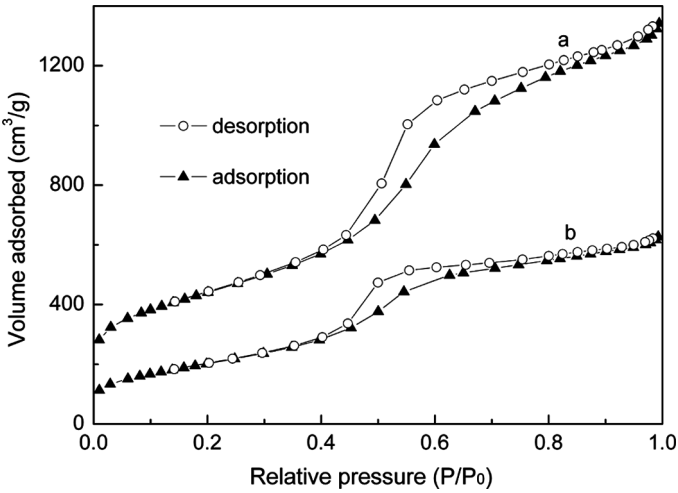

Figure 3. N_2 adsorption/desorption isotherms for (a) CMK-3 and (b) PANI/CMK-3.

The WXRD patterns of PANI and PANI/CMK-3 are given in Figure 2, inset. The XRD pattern of PANI/CMK-3 shows the broad peak of the amorphous wall structure of mesoporous carbon, but no appreciable peak of PANI is observed, which supports the fact that PANI has been almost confined in the pores rather than deposited on the surface of the mesoporous carbon and its crystallization is hindered due to the confinement effect.[27]

The structure effects of PANI intercalation were investigated by N_2 adsorption measurement. Figure 3 illustrates the N_2 adsorption/desorp-desorption isotherms of the studied samples. Both samples exhibit type IV isotherms with hysteresis loops, which is a typical characteristic of mesoporous materials.[28] The sharp inflection in the range of $P/P_0 = 0.4$–0.8, corresponding to capillary condensation of N_2, indicates the uniformity of the pores. The main structural characteristics of the samples are listed in Table 1. The CMK-3 sample exhibits a high surface area of $1217\,m^2/g$, a pore volume of $1.53\,cm^3/g$, and a pore size distribution centered around 4.6 nm. These values are close to the previous reports for CMK-3 material.[23] After inclusion of PANI in the mesopores, the surface area, pore volume, and average pore size decrease to $930\,m^2/g$, $0.99\,cm^3/g$, and 4.2 nm, respectively, also suggesting that most pores have been filled with polymer.

In order to determine the morphology and ordered structure of PANI/CMK-3 nanocomposite, SEM and TEM studies were also carried out, as shown in Figure 4. The PANI/CMK-3 composite shows rod-like

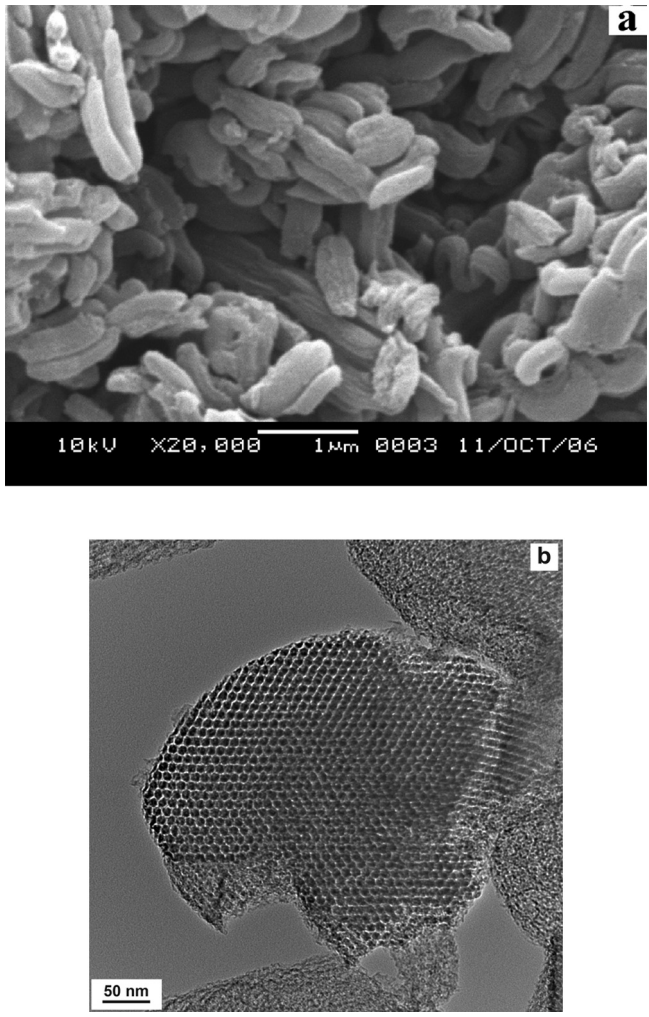

Figure 4. (a) SEM image of PANI/CMK-3 nanocomposite and (b) HRTEM image of PANI/CMK-3 nanocomposite taken with the incident electron beam parallel to the direction of the channels.

morphology, and no appreciable PANI particles on the surface of CMK-3 are observed in Figure 4(a), while Figure 4(b) clearly demonstrates that the PANI/CMK-3 possesses well-defined hexagonally ordered mesostructure after inclusion of PANI in the channels of CMK-3. Furthermore, according to the images, the pore size can be estimated to be $4 \sim 5$ nm, which is close to the value of the pore diameter calculated by the BJH method (Table 1).

Table 1. Structural characteristics of SBA-15, CMK-3, and PANI/CMK-3 samples

Samples	Unit cell parameter (nm)	Surface area (BET) (m^2/g)	Pore diameter (BJH) (nm)	Pore volume (BJH) (cm^3/g)
SBA-15	10.7	580	8.7	1.08
CMK-3	10.0	1217	4.6	1.53
PANI/CMK-3	9.8	930	4.2	0.99

The presence of PANI in the nanocomposite can be confirmed directly by FT-IR spectra analysis, as shown in Figure 5. The IR spectrum of PANI/CMK-3 reveals the characteristic absorption peaks of PANI other than that of mesoporous carbon. The peak at 3425 cm^{-1} is due to the N−H stretching vibrations overlapped by the −OH groups from the CMK-3, while C=N and C=C stretching vibrations for the quinonoid and benzenoid ring are centered at 1582 and 1503 cm^{-1}, respectively. This result indicates that protonated PANI has been synthesized in the nanocomposite.

Figure 6 presents the Raman spectra of PANI, CMK-3, and PANI/CMK-3 samples. For pure PANI, the peaks at 1164, 1342, 1489, and 1596 cm^{-1} can be assigned to C−H bending of the quinonoid ring, $C-N^+$ stretching, C=N stretching, and C−C stretching vibration of benzene ring, revealing the presence of the doped PANI structure.[29] For CMK-3 materials, two broad Raman peaks at 1344 and 1598 cm^{-1}

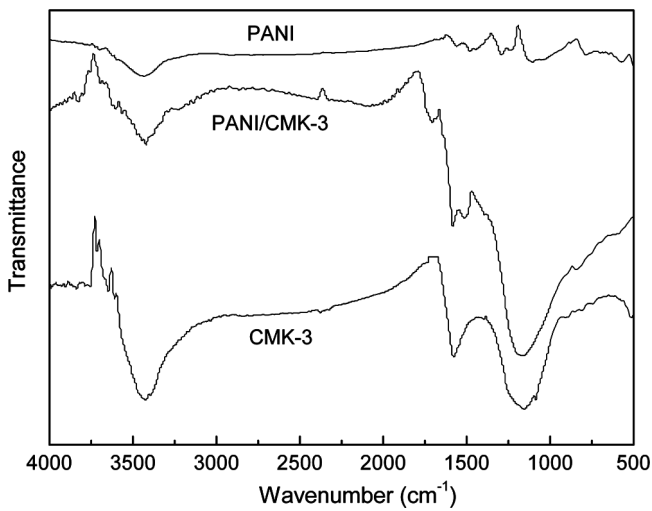

Figure 5. FT-IR spectra of CMK-3, PANI, and PANI/CMK-3.

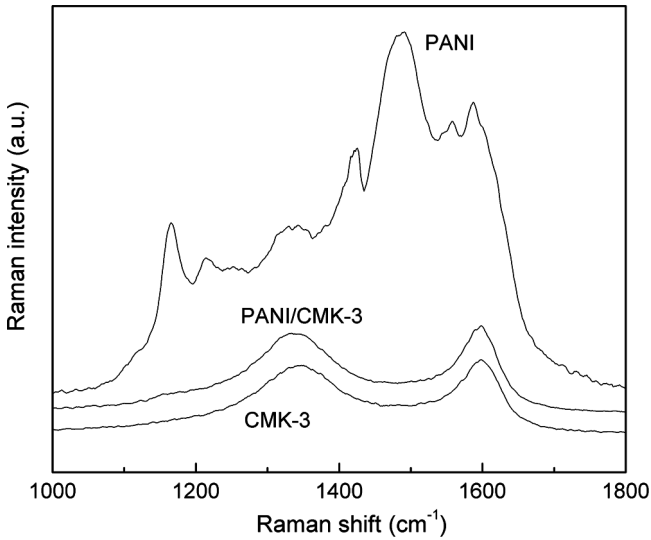

Figure 6. Raman spectra of PANI, CMK-3, and PANI/CMK-3.

suggest the atomically disordered nature of the carbon frameworks.[23] It is worth noting that the spectrum of PANI/CMK-3 is nearly identical to that of CMK-3 but different from that of PANI. However, in recent studies on PANI/carbon nanotube composites,[30] the Raman spectrum of the composites was found to be almost the same as that of PANI when PANI was coated on the surface of a carbon nanotube. Accordingly, it could be further inferred that PANI is incorporated in the mesopores of CMK-3 in our experiment.

Further evidence of the presence of polymer in the nanocomposite was confirmed by TGA as shown in Figure 7. The PANI demonstrates three-step weight loss. The initial loss is mainly attributed to the elimination of residual water, and the second loss, from 170° to 300°C, is due to the removal of dopant molecules; the third loss, starting beyond 400°C, is caused by the decomposition of PANI chains.[31] However, it is worth noting that the PANI/CMK-3 nanocomposite does not have a distinct decomposition temperature and shows a gradual weight loss with increasing temperature. The results imply good thermal stability of PANI in the nanocomposite because of diffusion constraints in the channel system.[19]

The electrical conductivities of PANI, CMK-3, and PANI/CMK-3 samples were measured with the standard van der Pauw DC four-probe method.[32] The conductivities of PANI doped with HCl and CMK-3 at room temperature are 1.0 and 1.40 S/cm, respectively. With encapsulated 8.4 wt% PANI in CMK-3, the conductivity of PANI/CMK-3 nanocomposite (0.78 S/cm) is lower than that of pristine CMK-3. This difference is

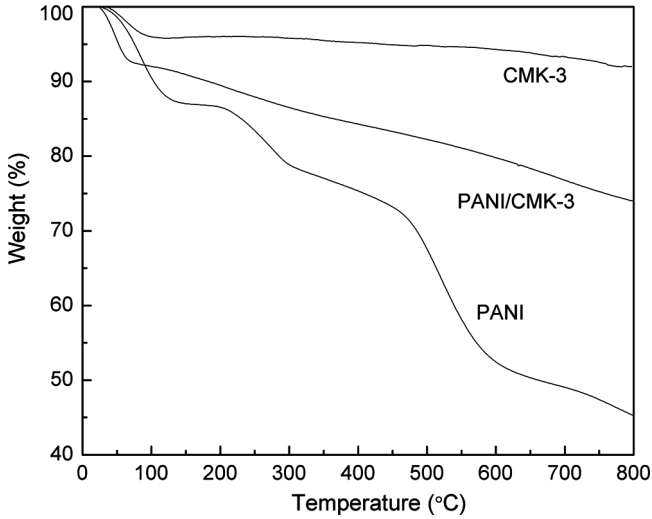

Figure 7. TGA curves of PANI, CMK-3, and PANI/CMK-3.

probably caused by electrical barriers provided by atomic defects in the CMK-3 host lattice.[12]

CONCLUSIONS

In summary, a new nanocomposite with PANI confined in the ordered mesoporous carbon CMK-3 has been successfully synthesized by chemical oxidative polymerization. The presence of PANI in the channels was confirmed by different characterization methods, and the resulting nanocomposite still retains the ordered mesostructure. The results also suggest that incorporation of PANI can effectively modify the surface chemistry of CMK-3.

REFERENCES

[1] Schmid, G., M. Baumle, M. Geerkens, I. Heim, C. Osemann, and T. Sawitowski. (1999). Current and future applications of nanoclusters. *Chem. Soc. Rev.* **28**, 179–185.

[2] Sawitowski, T., Y. Miquei, A. Heilmann, and G. Schmid. (2001). Optical properties of quasi one-dimensional chains of gold nanoparticles. *Adv. Funct. Mater.* **11**, 435–440.

[3] Vallet-Regi, M., A. Ramila, R. P. Real, and J. P. Pariente. (2001). A new property of MCM-41: Drug delivery system. *Chem. Mater.* **13**, 308–311.

[4] Zhang, L. X., J. L. Shi, J. Yu, A. L. Hua, X. G. Zhao, and M. L. Ruan. (2002). A new in-situ reduction route for the synthesis of Pt nanoclusters in the channels of mesoporous silica SBA-15. *Adv. Mater.* **14**, 1510–1513.
[5] Wang, Y. M., Z. Y. Wu, L. Y. Shi, and J. H. Zhu. (2005). Rapid functionalization of mesoporous materials: Directly dispersing metal oxides into as-prepared SBA-15 occluded with template. *Adv. Mater.* **17**, 323–327.
[6] Lee, K. P., A. P. Showkat, A. I. Gopalan, S. H. Kim, and S. H. Choi. (2005). Synthesis of poly(diphenylamine) nanotubes in the channels of MCM-41 through self-assembly. *Macromolecules* **38**, 364–371.
[7] Zhu, S., H. Zhou, M. Hibino, I. Honma, and M. Ichihara. (2005). Synthesis of MnO_2 nanoparticles confined in ordered mesoporous carbon using a sonochemical method. *Adv. Funct. Mater.* **15**, 381–386.
[8] Wikander, K., A. B. Hungria, P. A. Midgley, A. E. C. Palmqvist, K. Holmberg, and J. M. Thomas. (2007). Incorporation of platinum nanoparticles in ordered mesoporous carbon. *J. Colloid Interface Sci.* **305**, 204–208.
[9] Huwe, H. and M. Froba. (2007). Synthesis and characterization of transition metal and metal oxide nanoparticles inside mesoporous carbon CMK-3. *Carbon* **45**, 304–314.
[10] Hartmann, M., A. Vinu, and G. Chandrasekar. (2005). Adsorption of vitamin E on mesoporous carbon molecular sieves. *Chem. Mater.* **17**, 829–833.
[11] Liu, X., L. Zhou, J. Li, Y. Sun, W. Su, and Y. Zhou. (2006). Methane sorption on ordered mesoporous carbon in the presence of water. *Carbon* **44**, 1386–1392.
[12] Kim, C. H., S. S. Kim, F. Guo, T. P. Hogan, and T. J. Pinnavaia. (2004). Polymer intercalation in mesostructured carbon. *Adv. Mater.* **16**, 736–739.
[13] Fuetres, A. B. (2005). Encapsulation of polypyrrole chains inside the framework of an ordered mesoporous carbon. *Macromol. Rapid Commun.* **26**, 1055–1059.
[14] Cho, M. S., H. J. Choi, K. Y. Kim, and W. S. Ahn. (2002). Synthesis and characterization of polyaniline/mesoporous SBA-15 nanocomposite. *Macromol. Rapid. Commun.* **23**, 713–716.
[15] Cho, M. S., H. J. Choi, and W. S. Ahn. (2004). Enhanced electrorheology of conducting polyaniline confined in MCM-41 channels. *Langmuir* **20**, 202–207.
[16] Cheng, Q., V. Pavlinek, A. Lengalova, C. Li, Y. He, and P. Saha. (2006). Conducting polypyrrole confined in ordered mesoporous silica SBA-15 channels: Preparation and its electrorheology. *Micropor. Mesopor. Mater.* **93**, 263–269.
[17] Sasidharan, M., N. K. Mal, and A. Bhaumik. (2007). In-situ polymerization of grafted aniline in the channels of mesoporous silica SBA-15. *J. Mater. Chem.* **17**, 278–283.
[18] Li, N., X. T. Li, W. C. Geng, T. Zhang, Y. Zuo, and S. L. Qiu. (2004). Synthesis and humidity sensitivity of conducting polyaniline in SBA-15. *J. Appl. Polym. Sci.* **93**, 1597–1601.

[19] Wu, C. G. and T. Bein. (1994). Conducting polyaniline filaments in a mesoporous channel host. *Science* **264**, 1757–1758.
[20] Takei, T., K. Yoshimura, Y. Yonesaki, N. Kumada, and N. Kinomura. (2005). Preparation of polyaniline/mesoporous silica hybrid and its electrochemical properties. *J. Porous Mater.* **12**, 337–343.
[21] Bissessur, R., P. K. Y. Liu, and S. F. Scully. (2006). Intercalation of polypyrrole into graphite oxide. *Synth. Met.* **156**, 1023–1027.
[22] Kim, B. H., J. H. Jung, J. W. Kim, H. J. Choi, and J. Joo. (2001). Physical characterization of polyaniline-Na^+-montmorillonite nanocomposite intercalated by emulsion polymerization. *Synth. Met.* **117**, 115–118.
[23] Jun, S., S. H. Joo, R. Ryoo, M. Kruk, M. Jaroniec, Z. Liu, T. Ohsuna, and O. Terasaki. (2000). Synthesis of new, nanoporous carbon with hexagonally ordered mesostructure. *J. Am. Chem. Soc.* **122**, 10712–10713.
[24] Zhao, D., J. Feng, Q. Huo, N. Melosh, G. H. Fredirckson, B. F. Chemlka, and G. D. Stucky. (1998). Triblock copolymer syntheses of mesoporous silica with periodic 50 to 300 angstrom pores. *Science* **279**, 548–552.
[25] Hampsey, J. E., Q. Hu, Z. Wu, L. Rice, J. Pang, and Y. Lu. (2005). Templating synthesis of ordered mesoporous carbon particles. *Carbon* **43**, 2977–2982.
[26] Lee, J., S. Yoon, S. M. Oh, C. H. Shin, and T. Hyeon. (2000). Development of a new mesoporous carbon using an HMS aluminosilicate template. *Adv. Mater.* **12**, 359–362.
[27] Cheng, Q., V. Pavlinek, C. Li, A. Lengalova, Y. He, and P. Saha. (2006). Synthesis and characterization of new mesoporous material with conducting polypyrrole confined in mesoporous silica. *Mater. Chem. Phys.* **98**, 504–508.
[28] Sing, K. S. W., D. H. Everett, R. A. W. Haul, L. Moscou, R. A. Pierotti, J. Rouquerol, and T. Siemieniewska. (1985). Reporting physisorption data for gas/solid system with special reference to the determination of surface area and porosity. *Pure Appl. Chem.* **57**, 603–619.
[29] Wei, Z., Z. Zhang, and M. Wang. (2002). Formation mechanism of self-assembled polyaniline micro/nanotubes. *Langmuir* **18**, 917–921.
[30] Wu, T. M. and Y. W. Lin. (2006). Doped polyaniline/multi-walled carbon nanotube composites: Preparation, characterization and properties. *Polymer* **47**, 3576–3582.
[31] Lee, D. and K. Char. (2002). Thermal degradation behavior of polyaniline in polyaniline/Na^+-montmorillonite nanocomposites. *Polym. Degradation Stab.* **75**, 555–560.
[32] Dai, L., J. Lu, B. Matthews, and W. H. Mau. (1998). Doping of conducting polymers by sulfonated fullerene derivatives and dendrimers. *J. Phys. Chem. B* **102**, 4049–4053.